Report No.
UCB/SEMM-2013/02

Structural Engineering
Mechanics and Materials

SHAKE-TABLE TEST RESPONSE OF A ROCKING POST-TENSIONED HyFRC BRIDGE COLUMN

By

William Trono, Gabriel Jen, Claudia Ostertag, and
Marios Panagiotou

February 2013

Department of Civil and Environmental Engineering
University of California, Berkeley

SHAKE-TABLE TEST RESPONSE OF A ROCKING POST-TENSIONED HYFRC BRIDGE COLUMN

William Trono[1)], Gabriel Jen[1)], Claudia Ostertag[2)], and Marios Panagiotou[3)]

1) PhD Candidate, Dept. of Civil and Environmental Engineering, University of California, Berkeley, CA
2) Professor, Dept. of Civil and Environmental Engineering, University of California, Berkeley, CA
3) Asst. Professor, Dept. of Civil and Environmental Engineering, University of California, Berkeley, CA
will.trono@berkeley.edu, gjen@berkeley.edu, ostertag@ce.berkeley.edu, panagiotou@berkeley.edu

Abstract: Conventional reinforced concrete bridge columns in high seismic regions are designed to be ductile during earthquakes; however, column damage and residual drift can cause bridges to remain out of service for extended periods during replacement or repair. In this study, a rocking post-tensioned HyFRC bridge column was designed to limit damage and residual drifts and was tested dynamically under earthquake excitation. The column utilized post-tensioned strands, hybrid fiber reinforced concrete (HyFRC), and a combination of unbonded and headed longitudinal reinforcement. HyFRC with a total of 1.5% micro and macro fibers by volume and headed steel reinforcement at a ratio of 1.5% (discontinuous at the foundation) were used in the precast end region to improve the behavior of the rocking interface under high compressive forces. The 1/3 scale cantilevered bridge column was subjected to a sequence of nine scaled ground motion records of increasing intensity chosen to produce specific ductility demands in a conventionally designed reference specimen. The column exhibited excellent re-centering capability and light damage in the HyFRC end region, reaching a drift of 8.0% with an accumulated residual drift of less than 0.4%. Compressive damage was controlled in the end region by the HyFRC and the headed reinforcement.

1. INTRODUCTION

Reinforced concrete bridge columns in seismic regions are designed to be ductile by forming plastic hinges to accommodate inelastic deformations during earthquakes. Code requirements are intended to prevent collapse of bridges under design seismic hazards; however, damage in column plastic hinge regions can cause bridges to be out of service during column repair or replacement (CalTrans 2010). Residual column drift ratios (drifts) are expected following earthquakes if concrete and reinforcing bars incur severe inelastic damage in the plastic hinge.

In this study, a bridge column was designed with an objective of reducing or eliminating residual drifts after earthquakes. This objective was satisfied by several unique design details. First, the column was designed to rock about the foundation to avoid plastic hinge formation by unbonding the flexural reinforcement near the column-foundation interface. Second, fully unbonded, post-tensioned steel strands provided axial pre-compression and overturning resistance. Finally, hybrid fiber reinforced concrete (HyFRC) and headed reinforcing bars (rebar) that terminated at the column-foundation interface were employed to reduce compressive damage during rocking.

The rocking, post-tensioned (RPT) HyFRC bridge column was subjected to dynamic excitation in three directions on the Pacific Earthquake Engineering Research Center's (PEER) Earthquake Simulator in Richmond, CA. Eleven scaled earthquake ground motion records were applied.

A reference column with conventional design details and equivalent geometry and inertial mass was tested using the same ground motion sequence for comparison. During the seventh motion, the reference column reached a drift of 10.8% but had a residual drift of 6.8% and testing was halted. The RPT HyFRC column reached a drift of 8.0% during the same motion but had a residual drift of less than 0.4%.

2. BACKGROUND

The equations of motion for slender, inverted pendulum-type structures (structures that can rock freely about their base) were first introduced by Housner (1963) who recognized their tendency to maintain stability during strong ground shaking. Since then, numerous experimental and analytical studies have verified rocking as an effective means of accommodating inelastic displacement demands in reinforced concrete structures during earthquakes. Rocking systems that utilize unbonded post-tensioning (PT) can have re-centering hysteretic response upon unloading and various methods have been employed to add hysteretic energy

dissipation to such systems in addition to re-centering.

2.1 Columns with Unbonded Post-tensioning and Bonded or Unbonded Mild Steel Reinforcing Bars

Many researchers have investigated the use of unbonded post-tensioning in concrete beam and column assemblages to provide re-centering hysteretic behavior (Mander and Cheng 1997, Cheng 2008). Often these assemblages consisted of precast concrete segments connected by post-tensioned strands (Hewes and Priestly 2002, ElGawady et. al. 2010, Billington and Yoon 2004). In all cases, overturning resistance was provided by the elastic response of the unbonded post-tensioned strands and caused origin-oriented hysteretic behavior upon unloading.

Several analytical studies have investigated the performance of bridge columns built with a combination of mild steel longitudinal reinforcement and unbonded post-tensioning which can provide both hysteretic energy dissipation and column re-centering (Kwan and Billington 2003, Sakai and Mahin 2004). Columns with higher proportions of unbonded post-tensioning showed a greater tendency to re-center but often caused crushing of concrete earlier due to higher compressive stresses. Columns with higher proportions of mild steel reinforcement showed more hysteretic energy dissipation.

Billington and Yoon (2004) showed that a ductile fiber reinforced cement-based composite (DFRCC), a class of high performance fiber reinforced cementitious composites (HPFRCC) that exhibits strain hardening behavior in uniaxial tension, provided more energy dissipation in such systems than normal concrete and maintained its integrity considerably better under high compressive loads. Even with modest transverse reinforcement, the DFRCC did not spall.

Jeong et. al. (2008) tested columns with unbonded mild steel reinforcement and unbonded post-tensioning and found that unbonding the mild steel resulted in a shorter plastic hinge region and lower strains in the bars.

2.2 Columns with Hybrid Fiber Reinforced Concrete

This study considers a column designed to rock containing a combination of unbonded post-tensioning strands and unbonded mild steel reinforcing bars. In addition, the column incorporates hybrid fiber reinforced concrete (HyFRC), a class of tensile strain hardening HPFRCC containing both steel macrofibers and polymer microfibers at a fiber volume fraction of 0.015, in the end region. This material was initially developed for lightly reinforced bridge approach slabs with a performance criterion of maintaining strain compatibility with mild steel reinforcement through the tensile yield strain of steel of 0.2% (Blunt and Ostertag 2009). The material was optimized to have self-compacting properties in the fresh state (SC-HyFRC) to ease placement in densely reinforced structures (Jen et. al. 2012).

Cyclic testing of columns built with HyFRC and unbonded longitudinal reinforcement with no post-tensioning showed less spalling and compressive damage compared to conventionally designed columns with twice the transverse reinforcement under the same drift demands (Panagiotou et. al. 2012, Kumar et. al. 2011). Furthermore, small-scale tests revealed greater post-peak compressive strength and stability in confined HyFRC compared to equally confined normal concrete (Trono et. al. 2011). HyFRC is utilized in this column to improve energy dissipation and compressive damage resistance in the end region where large compressive forces are expected.

2.3 Headed Reinforcement Terminating at the Column-Foundation Interface

In addition to using HyFRC, a second detail which differentiates this column design from previous tests on columns with unbonded post-tensioning and unbonded mild steel reinforcement is the inclusion of headed compression-only reinforcing bars which terminated at the column-foundation interface. The 51x51x13 mm steel plate heads reinforce and confine the HyFRC at the column-foundation interface. Holden et. al. (2003) used a similar design in a precast pre-stressed concrete wall, lining the base of the wall with a steel plate and adding additional plates to the extreme ends of the wall at the base. Belleri et. al. (2013) used headed bars which terminated at the foundation of a rocking wall for the same purpose. To the authors' knowledge, this type of detailing has not been tested in post-tensioned columns, although another column in this test bed had similar detailing (Restrepo and Guerrini 2012).

3. TEST PROGRAM

The RPT HyFRC column was tested as part of PEER's Damage Resistant Re-centering Bridge Columns test bed, a collaborative project from three universities consisting of three different advanced bridge column specimens as well as a reference column with conventional design details for comparison. All four columns had equivalent inertial mass and geometry and were subjected to the same sequence of scaled earthquake ground motion records. This report focuses on the experimental response of the RPT HyFRC column and draws comparisons with the response of the reference specimen.

3.1 RPT HyFRC Column Design Objectives

There were three specific objectives in the design of the RPT HyFRC column: (1) Minimize or eliminate the likelihood of residual column drifts for imposed drift demands up to 7%, (2) Limit inelastic compression damage at the rocking interface, and (3) Ensure that the post-tensioning remains elastic and prevent fracture of the continuous reinforcement at 7% drift.

To reach these objectives, the proportion of unbonded rebar to axial load (from post-tensioning and inertial mass) was optimized to encourage column re-centering and achieve the target lateral strength. HyFRC and headed reinforcement that terminated at the rocking interface were employed to control inelastic compressive damage at the rocking toe. In addition, the post-tensioning was designed to remain elastic up to column drifts of 7%, and the continuous

longitudinal steel was unbonded over a length sufficient to prevent fracture at 7% drift. Preliminary column design and analysis was conducted using an analytical model built in OpenSEES, but details of the model are not included herein.

3.2 Description of Test Specimens

Details of the RPT HyFRC column and the reference column are shown in Figure 1 and Figure 2, respectively. The design of flexural reinforcement and post-tensioning in the rocking column was chosen to achieve approximately the same lateral strength and stiffness as the reference column. The length scale factor for both specimens was 3.

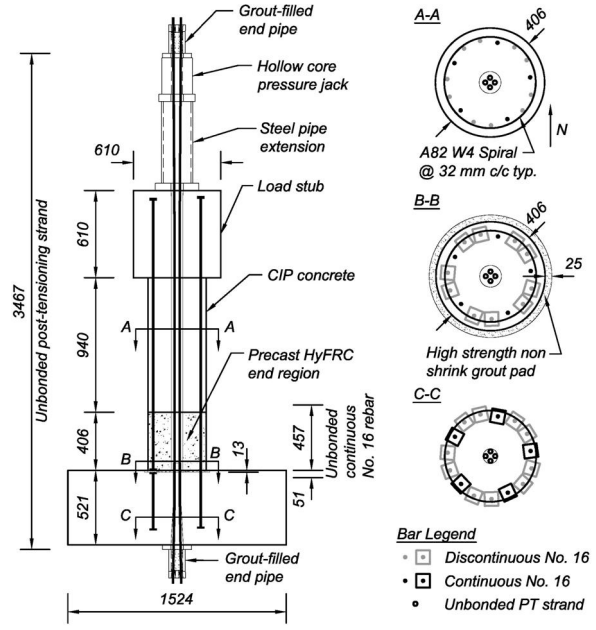

Figure 1 Rocking Post-tensioned HyFRC Column Elevation and Cross Sections

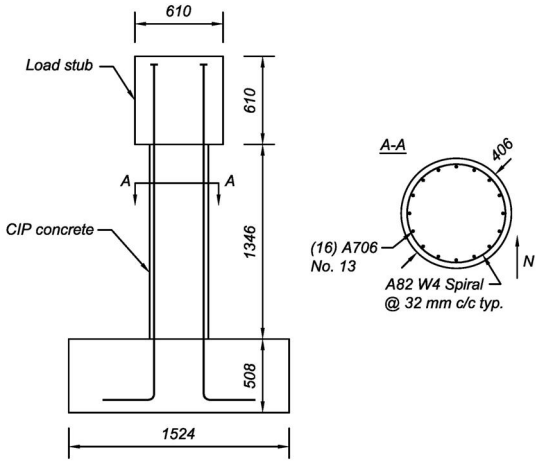

Figure 2 Reference Column Elevation and Cross Section

The RPT HyFRC column contained 15 ASTM A706 Grade 420 No. 16 bars longitudinally. Five of these bars continued from the column into the foundation and were unbonded over the length shown using tightly wrapped duct tape coated with lithium grease. The remaining ten bars terminated at the column-foundation interface with 51x51x13 mm steel heads and were fully bonded to the concrete. Four 15.2 mm dia. ASTM A416 Grade 1860 seven wire strands ran through a corrugated metal duct in the center of the column and were unbonded between their anchorages. As shown in Figure 1, a steel pipe was used to increase the unbonded length of the PT to reduce the chance of yielding the strands (in an actual bridge, the PT could be anchored within the superstructure). The longitudinal steel effective in flexure consisted of the five unbonded No. 16 bars and the four PT strands for a total effective volumetric ratio of $\rho_{l,eff}$ = 1.2%. The volumetric ratio of the discontinuous headed bars terminating at the column-foundation interface was 1.5%. Transverse shear and confinement reinforcement was provided by an ASTM A82 W4 steel spiral (5.7 mm dia.) at 32 mm spacing, for a volumetric ratio of ρ_s = 0.9%. The spiral was discontinuous between the base of the column and the foundation.

The end region was precast with HyFRC and installed onto a wet-set grout pad on the top of the foundation (see Figure 1). The precast element contained ten discontinuous No. 16 headed bars as well as PVC and corrugated metal ducts for the continuous No. 16 bars and PT strands, respectively. No. 16 double-headed bars were also cast in the foundation in the same pattern as the discontinuous bars in the precast end region and terminated at the top of a 13 mm recession in the top of the foundation. These bars acted to distribute the compression from the column above into the foundation (with the high strength grout pad between).

Installation of the precast piece consisted of feeding the five continuous No. 16 bars (which were embedded in the foundation) through the PVC ducts in the precast piece, pouring the wet high strength non-shrink grout into the recession in the top of the foundation, and finally lowering the piece onto the wet grout pad, allowing it to rest on 10 mm shims while the grout cured. Grout was then poured into the void space in the PVC ducts to provide buckling resistance to the unbonded bars.

The remainder of the column was cast in place with normal concrete. Six days prior to testing, the four PT strands were stressed individually to 48% of their yield strength for a total PT force of 455 kN. The end wedge anchor plates fit into specially fabricated steel pipe sections which were filled with grout to a depth of 10 strand diameters (152 mm) after stressing in order to eliminate stress concentrations at the wedge anchors that could lead to premature strand failure. Weld beads on the inside surface of the pipe allowed any increase in strand tensile force during testing to develop in the grout away from the anchorage.

The reference column (Figure 2) was designed with a longitudinal volumetric steel ratio of ρ_l = 1.6% consisting of 16 ASTM A706 Grade 420 No. 13 bars. Transverse reinforcement was continuous into the foundation and consisted of the same A82 W4 smooth steel spiral at the same spacing as the RPT HyFRC column for a spiral volumetric ratio of ρ_s = 0.9%.

3.3 Specimen Material Properties

The HyFRC used in the precast end region of the RPT HyFRC column contained hooked-end steel fibers at 1.3% by volume with a length of 30 mm, a diameter of 0.55 mm, and a yield strength of 1100 MPa. It also contained polyvinyl alcohol (PVA) fibers at 0.2% by volume with a length of 8 mm, a diameter of 0.04 mm, and a yield strength of 1600 MPa. Two chemical admixtures, superplasticizer (SP) and viscosity modifying admixture (VMA), were used to improve the workability of the fresh mix. The material proportions of HyFRC are given in Table 1.

Table 1 HyFRC Material Mix Proportions

kg per cubic meter				*fiber volume %*	
Water	Cement[a]	Fly Ash[b]	Gravel[c]	Steel	PVA
219	*413*	*136*	*418*	*1.3*	*0.2*
Sand[d]	SP	VMA			
1044	*2.3*	*5.6*			

[a]ASTM C150 Type II; [b]ASTM C618 Type C; [c]pea gravel, 9.5 mm MSA; [d]coarse sand, FM = 3.2

The compressive strengths, f_c', of the normal cast-in-place concrete used for the columns and the foundations, the HyFRC, and the high strength non-shrink grout pad are given in Table 2. Concrete and HyFRC compressive strengths were averaged from three 152x304 mm cylinders, while high strength grout strengths were averaged from five 51x51x51 mm cubes.

Table 2 Compressive Strength of Column Materials

	Sampled f_c' (MPa)			
Specimen	*Column*	*Found.*	*HyFRC*	*Grout*
RPT HyFRC	34.5	55.5	44.6[b]	63.8
Reference	22.6[a]	34.7	-	-

[a] 18% lower than design f_c' = 27.6 MPa
[b] average strain at f_c' equal to 0.35%

The A706 No. 16 reinforcing bars used in the RPT HyFRC specimen had an average tested yield strength of 481 MPa and an ultimate strength of 658 MPa. Their tensile stress-strain response is shown in Figure 3(a). The A416 strands had an average tested yield strength of 1704 MPa and a breaking strength of 1874 MPa as shown in Figure 3(b). Finally, the A706 No. 13 bars used in the reference column had an average tested yield strength of 433 MPa and an ultimate strength of 651 MPa as shown in Figure 3(c). In all three cases, strain was measured over 51 mm, stress was calculated assuming nominal cross sectional area, and three coupons of each material were tested. Figure 3(d) shows the stress-strain response of the A82 W4 spiral (after straightening a circularly-deformed sample).

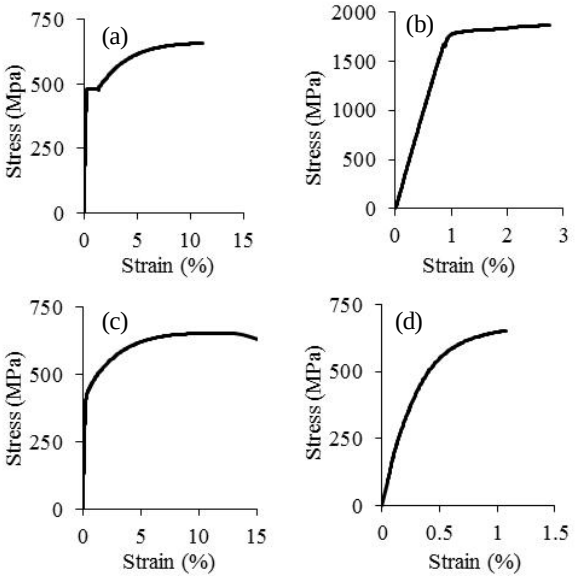

Figure 3 Tensile Stress-Strain Response of (a) A706 No. 16 bars, (b) A416 PT Strand, (c) A706 No. 13 bars, and (d) A82 W4 spiral

3.4 Test Configuration and Instrumentation

The same test setup was used on the shaking table for both the RPT HyFRC column and the reference column and is shown in Figure 4. Inertial mass was applied in the form of three 3048x3048x356 mm reinforced concrete plates. Wide flange steel cantilevered beams were fixed to the column load stub and the mass plates were fixed to the wide flange steel beams using post-tensioned bars. The total inertial mass applied to the columns was approximately 24500 kg (for a gravity load of 240 kN), and the center of mass was found to be 2438 mm above the top of the foundation. The axial load ratios for RPT HyFRC and reference columns, defined as the gravity load divided by $f_c'A_g$, where f_c' was the tested compressive strength of the column's normal concrete and A_g the gross cross sectional area, were 5.4% and 8.2%, respectively.

Instrumentation for the RPT HyFRC column consisted of five load cells, 30 displacement transducers, and 41 strain gages. Four load cells, 32 displacement transducers, and 54 strain gages were used for the reference column. Thirty-five accelerometers and 21 wire potentiometers were used for both columns. All instruments were sampled at 200 Hz.

Each of the column foundations was fixed upon four tri-axial load cells that measured shear force in two directions and axial force (see Figure 4). The RPT HyFRC column also had a fifth load cell in the form of a hollow core pressure jack (with a pressure transducer) in series with the post-tensioning to measure the PT force during testing.

In both tests, accelerometers were fixed to the foundation, column, and mass plates in both the horizontal and vertical directions at multiple locations. Displacement transducers were fixed to rods embedded in the columns on four sides at discrete heights to estimate the curvature profiles during testing. Seven groups of three wire potentiometers tracked the 3-D displacement at seven points on the specimen—three on the foundation and four on the

mass plates. These displacements were used to resolve three translations and three rotations at the center of mass using the procedure presented in Vithani and Gupta (2002).

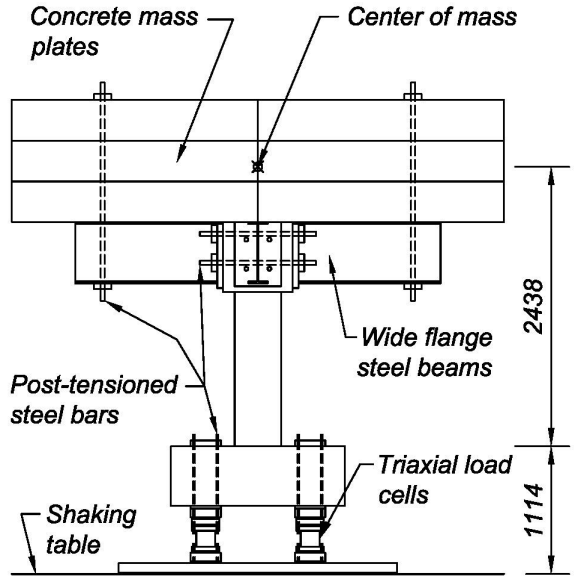

Figure 4 Shaking Table Test Setup

3.5 Shaking Table Test Sequence

A sequence of nine scaled earthquake ground motion records, each with North-South (NS), West-East (WE), and vertical direction components, was chosen by the research group for testing of the RPT HyFRC column, the reference column, and the other columns of the Damage Resistant Re-centering Bridge Columns test bed. Details of each record are given in Table 3. Priority was given to records that satisfied the following criteria: (1) They imposed similar displacements in all test bed columns over the fundamental period range 0.4 to 0.7 seconds, (2) They contained velocity pulses likely to cause large column drifts, and (3) They were generated by strike-slip fault mechanisms.

Time was scaled by $L^{-1/2}$ in order to maintain a scale factor of unity for induced accelerations (the length scale factor, L, was 3). Acceleration values (3 components) were also scaled by a constant for each signal so as to impose specific displacement ductility targets, μ, in the reference column (see Table 3) and comparable peak drifts in all test bed columns. The design level earthquakes were selected to impose a target displacement ductility of 4 (EQ4 and EQ5) to be consistent with the maximum design demand for single column bridge bents according to Caltrans SDC (2010). Some motions were filtered to remove displacement pulses that exceeded the shaking table's limits. Testing of the reference column was stopped after EQ7 due to substantial residual column drift. The RPT HyFRC column was subjected to two additional unplanned ground motions after the first nine since damage and residual drifts had been well controlled during the initial test sequence. Details of these motions are also included in Table 3.

White noise tests (table motions consisting of randomly generated, tri-directional, small-amplitude displacements) were run before each earthquake test for both columns to induce column vibration and evaluate the natural period as damage developed. Prior to the start of any dynamic testing, free vibration tests were performed on both columns by applying a static lateral load and quickly releasing it.

Table 3 Details of Earthquake Tests

Test	Earthquake[a] *Station*	Accel. SF	Target μ (ref. col.)
EQ1	Coalinga 1983/05/09 02:49 *46T07 Harris Ranch - Hdqtrs*	2.50	elastic
EQ2	Imperial Valley - 06 1979 *EC Meloland Overpass FF*	0.80	2
EQ3	Morgan Hill, 1984 *Coyote Lake Dam (SW Abut)*	0.70	2
EQ4[b]	Northridge - 01 1994 *Rinaldi Receiving Station*	0.56	4
EQ5[b]	Northridge - 01 1994 *Sylmar - Olive View Med FF*	-0.80	4
EQ6	Northridge - 01 1994 *Rinaldi Receiving Station*	0.90	6
EQ7	Kobe, Japan, 1995 *Takatori*	0.77	8
EQ8	Kobe, Japan, 1995 *Takatori*	-0.90	9.6
EQ9	Northridge - 01 1994 *Sylmar - Olive View Med FF*	-0.80	4
EQ10	Kobe, Japan, 1995 *Takatori*	0.90	-
EQ11	Northridge - 01 1994 *Rinaldi Receiving Station*	1.17	-

[a] *from PEER Ground Motion Database (2000, 2012)*
[b] *Design level earthquake*

4. TEST RESULTS

Dynamic testing confirmed that the RPT HyFRC column achieved its primary objective of minimizing residual column drifts compared to a conventionally designed column. The post-tensioned strands remained elastic and provided enough overturning resistance to re-center the column throughout testing, while the combination of headed compression-only reinforcement and HyFRC in the precast end region limited inelastic compressive damage. Fracture of the continuous unbonded reinforcement was delayed until the eleventh earthquake test when two bars fractured.

4.1 Measured Peak and Residual Column Drifts

Table 4 shows the peak drifts of the RPT HyFRC and reference specimens measured during testing as well as the

residual drifts measured at the end of each test. Figure 5 shows the same data side by side for the first seven EQ tests which were run on both columns. As shown, the RPT HyFRC column showed near perfect re-centering after the first five earthquake tests with residual drifts under 0.1%, even after reaching 4.3% drift during EQ4 and 6.2% drift during EQ5. During EQ7, the RPT HyFRC column reached a drift of 8.0%, but the residual drift remained less than 0.4%. During EQ11, when the column reached 8.8% drift, two unbonded bars fractured but the residual drift was still only 0.9%. Figure 6(a) shows the RPT HyFRC column after EQ11 at the end of testing.

The reference column developed a residual drift of 0.9% after the first five earthquakes, reaching a peak drift of 3.7% during EQ4 and 5.8% during EQ5 (the design level events). Further testing resulted in increased residual drifts in the reference column; EQ6 caused a drift of 6.1% and increased the residual to 1.6%, while EQ7 induced the largest drift of 10.8% which left a residual of 6.8%. Figure 6(b) shows the reference column after EQ7.

Table 4 Measured Peak and Residual Column Drifts

	RPT HyFRC Drift[a] (%)		Reference Drift[a] (%)	
Test	peak	residual	peak	residual
EQ1	0.5	0.0	0.4	0.0
EQ2	2.1	0.1	3.5	0.4
EQ3	2.1	0.1	1.5	0.4
EQ4	4.3	0.1	3.7	0.3
EQ5	6.2	0.1	5.8	0.9
EQ6	5.0	0.2	6.1	1.6
EQ7	8.0	0.4	10.8	6.8
EQ8	6.8	0.4	-	-
EQ9	7.2	0.6	-	-
EQ10	7.2	0.6	-	-
EQ11	8.8	0.9	-	-

[a]*Resultant value in NS, WE directions*

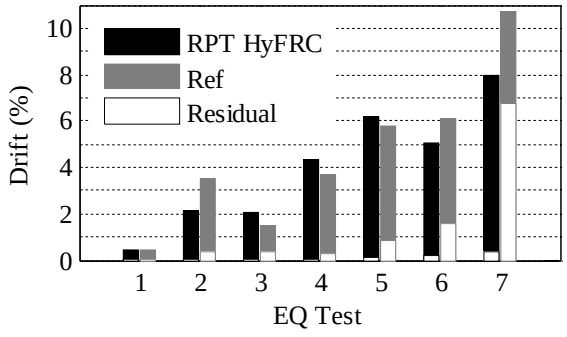

Figure 5 Peak and Residual Drift Comparison of the RPT HyFRC and Reference Column through EQ7

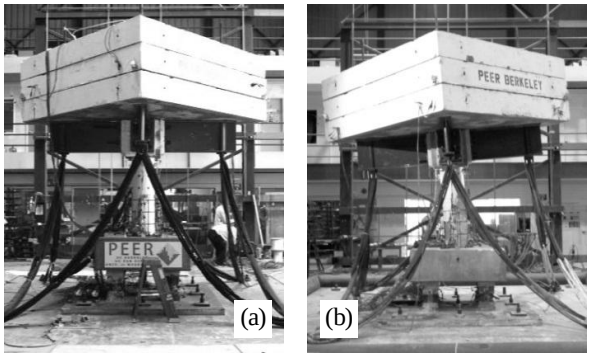

Figure 6 East Elevation after Testing, (a) RPT HyFRC Column at 0.9% Residual Drift after EQ11, (b) Reference Column at 6.8% Residual Drift after EQ7

4.2 Measured Base Rotation and Rocking Behavior

The RPT HyFRC column was designed to rock about its foundation in order to avoid damage caused by formation of a plastic hinge. Inelastic lateral drifts were accommodated by uplift of the column at the interface with the foundation rather than distributed tensile cracking. This mechanism was verified by comparing the measured base rotations to the lateral drift at the center of mass. Uplift from the foundation was measured by displacement transducers mounted to the column at heights of 52, 64, 67, and 49 mm above the foundation on the N, E, S, and W column faces, respectively. Base rotations, θ_b, in the N-S and W-E directions were calculated as the difference in opposite displacement transducer measurements divided by the horizontal distance between the transducers.

Figures 7(a) and 7(b) show the calculated base rotation plotted against drift of the center of mass in the N-S direction for EQ4 and EQ7 where the column reached peak drifts of 4.3% and 8.0%, respectively. The rocking mechanism is clearly illustrated by the fact that the inelastic column drifts are accommodated almost completely by rotation at the base.

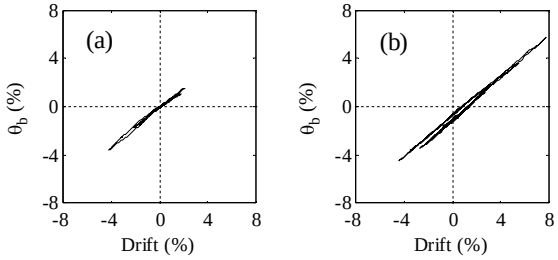

Figure 7 Measured Base Rotation vs. Drift in the NS Direction (N positive) for (a) EQ4 and (b) EQ7

4.3 Measured Overturning Moment vs. Drift Behavior

The hysteretic overturning moment vs. drift response in the N-S direction is shown in Figures 8(a), 8(b), and 8(c) for EQ4, EQ5, and EQ7, respectively. The figures on the left show the response of the reference column, while the figures on the right show the response of the RPT HyFRC column.

The overturning moment was calculated from load cell axial force measurements, corrected for the inertia of the foundation, and normalized by the weight of the inertial mass times the center of mass height.

As shown in Figure 8, the lateral strength of both columns was approximately equal, with inelastic response developing at an overturning moment of approximately 0.3WH. The response shown during EQ4 in Figure 8(a) clearly illustrates the re-centering effect in the RPT HyFRC column (right) as compared to the reference column (left); the reference column unloads and has a residual drift while the RPT HyFRC column unloads through the origin.

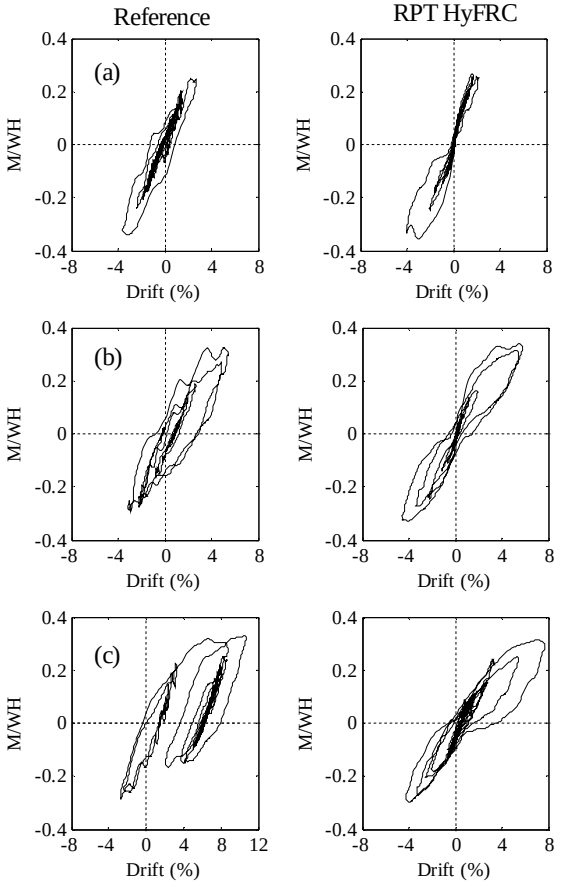

Figure 8 Measured Overturning Moment vs. Drift in the NS Direction for (a) EQ4, (b) EQ5, and (c) EQ7

During EQ5, the reference column reached a peak drift of 5.8% and developed more damage as evidenced by the wider hysteretic loop in the left side of Figure 8(b). In the right side of Figure 8(b), the response of the RPT HyFRC column continues to tend toward the origin upon unloading with only small drifts at zero overturning moment.

Finally, during EQ7, the reference column saw a peak drift of 10.8% and developed a significant residual drift as shown in the left side of Figure 8(c). The hysteretic loop of the RPT HyFRC column widened slightly during EQ7, but the column still re-centered upon unloading as shown in the right side of Figure 8(c).

4.4 Measured Load in the PT Strands

Prior to EQ1, the initial PT load in the RPT HyFRC column was 455 kN (48% yield). By the start of the final test, EQ11, the PT load had only decreased to 432 kN (45% yield) for an accumulated loss of only 5% of the initial load through the duration of all prior tests. The axial force provided by the PT was in addition to the 240 kN inertial mass from the concrete plates. The maximum PT force measured during all tests was 589 kN (62% of yield) which occurred during EQ7. Although there was a slight loss of PT force due to shortening of the column, the strands remained elastic through the duration of testing.

4.5 Measured Peak Tensile and Compressive Strains in the Reinforcing Bars of the RPT HyFRC Column

Table 5 shows the peak compressive strain, ε_c, and tensile strain, ε_t, as measured by strain gages fixed to bars B7 and U1, respectively, during each test. The location of these bars in the RPT HyFRC column cross section is given in Figure 9. The gage on bar B7 was fixed to the bar facing inward at a height 37 mm above the top of the foundation, while the gage on bar U1 was fixed to the bar facing outward at a height 76 mm above the foundation. Table 5 also shows the measured peak drift in the N direction during each EQ test. Drifts in the N direction caused tension in the unbonded bar U1 and compression in the discontinuous headed bar B7.

Table 5 Measured Peak Strains in Bars B7 and U1

Test	Peak Drift N-dir (%)	Peak ε_c Bar B7 (%)	Peak ε_t Bar U1 (%)
EQ1	0.5	-0.05	0.08
EQ2	2.1	-0.11	1.80
EQ3	1.7	-0.16	1.66
EQ4	2.2	-0.13	1.97
EQ5	5.9	-1.79	3.28
EQ6	4.5	-1.92	2.74
EQ7	7.8	-3.14	3.37
EQ8	6.6	-3.64	2.87
EQ9	7.1	-4.04	3.62
EQ10	6.9	-4.10	-
EQ11	8.0	-4.49	-

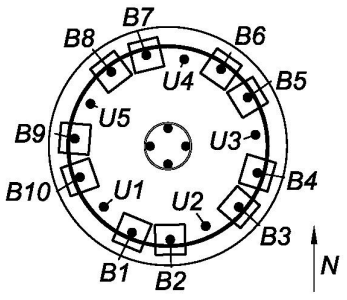

Figure 9 Reinforcing Bar Designations

As shown in Table 5, strains in the unbonded bar U1 were well-controlled by the unbonding of the bar from the surrounding concrete. As the column rocked and reached drifts of 5.9%, 7.8%, and 7.1% in the N direction during EQ5, EQ7, and EQ9, respectively, the measured peak tensile strain in bar U1 remained under 4%. The imposed drift during these tests was accommodated by uplift at the foundation (see Figure 7) and the low strain measurements in Bar U1 confirm that the uplift was distributed as strain over the unbonded length.

The discontinuous headed bars relieved the compressive forces imposed on the precast HyFRC during rocking as evidenced by the high recorded compressive strains in Table 5. Bar B7 yielded in compression, reaching a strain of -1.79%, when the column reached a peak drift of 5.9% in the N direction during EQ5. After yielding, inelastic compressive strains continued to increase during all subsequent tests. Strain gages on the other discontinuous bars B1, B3, B5, and B9 recorded peak compressive strains (over all tests) of 2.4%, 5.7%, 6.0%, and 2.0% but showed no evidence of buckling, and the spiral remained intact through the duration of testing.

4.6 Observed RPT HyFRC Column Damage

As shown by the measured test data, damage to the precast end region of the RPT HyFRC column was limited during testing; the PT strands remained elastic, the unbonded bars avoided fracture during the first ten EQ tests, and the precast end region maintained its integrity with no evidence of bar buckling or spiral fracture and only minor spalling.

The crack at the rocking plane first opened during EQ1 but was only captured in real-time by video cameras mounted on the foundation and was not apparent after the column re-centered. During EQ2, the crack at the rocking plane opened further and inspection showed light compressive scaling/cracking of the HyFRC and grout pad on the NE face of the column as shown in Figure 10(a) approximately 25 mm above the foundation. This cracking progressed slightly after EQ3, as shown in Figure 10(b).

The gap opening at the rocking interface opened significantly during EQ4 and EQ5 as shown in photos of the NE and SE faces of the column in Figure 10(c) and 10(d), respectively. These photos are taken from video of the response when the specimen was at 4.3% drift in the S direction for EQ4 and 6.2% drift in the N direction for EQ5, but in both cases the gap closed and the column re-centered. Figure 10(c) shows that some vertical splitting cracks initiated during EQ3, branching off the compressive cracks on the NE face. Figure 10(d) shows additional compressive cracking on the SE face at a height of approximately 64 mm above the foundation after EQ4.

The HyFRC remained intact with little to no spalling as shown on the four faces of the column in Figure 11(a) through 11(d) after the column reached 8.0% drift in the N direction during EQ7. Vertical splitting cracks that had initiated in prior tests propagated upward but did not extend higher than 200 mm above the foundation. Slight outward bulging of the column base was observed, yet neither spiral fracture nor bar buckling were evident on any face.

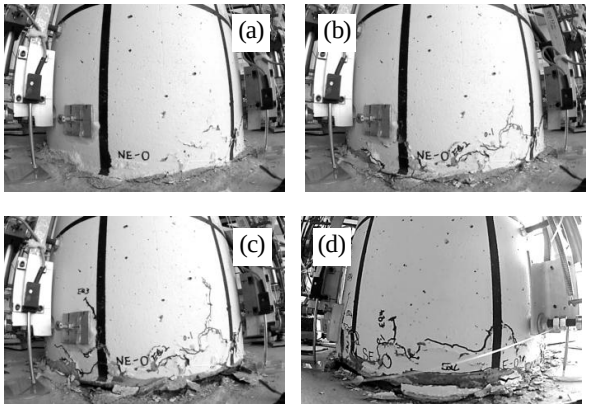

Figure 10 Damage to the Precast HyFRC End Region, (a) NE face after EQ2, (b) NE face after EQ 3, (c) NE face at 4.3% peak drift during EQ4, and (d) SE face at 6.2% peak drift during EQ 5

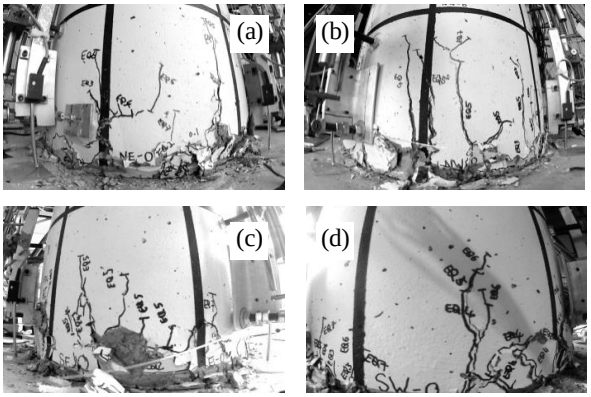

Figure 11 Damage to the Precast HyFRC End Region after EQ7, (a) NE face, (b) NW face, (c) SE face, and (d) SE face

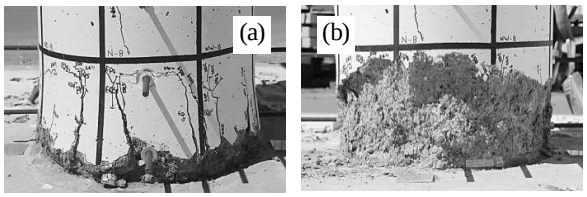

Figure 12 Final RPT HyFRC Damage State, N face (a) before and (b) after damaged HyFRC was removed

Fracture of the unbonded longitudinal bars was delayed until EQ11 when bars U1 and U4 fractured. Even after EQ11, the column residual drift was less than 1%. Figure 12(a) shows the damage state of the N face of the column at the end of testing after instrumentation had been removed. The HyFRC material did not spall from the column face during testing due to the fibers' ability to hold the material together even after splitting and compression cracks had formed. Following testing, damaged HyFRC was removed from the column face manually with a hammer and chisel as shown in Figure 12(b). After the material was removed, it was evident that damage was limited to cover HyFRC below

a height of 200 mm above the foundation and did not penetrate into the HyFRC core confined by the spiral.

4.7 Observed Reference Column Damage

The reference column accommodated the imposed drifts by distributed flexural cracking and eventual plastic hinge formation as imposed drifts increased.

Flexural cracks at spacings between 50 and 125 mm formed up to a height of approximately 600 mm above the foundation after EQ2 when the column reached 3.5% drift and are shown on the NE and NW faces of the column in Figures 13(a) and 13(b), respectively. After EQ6, compression damage in the form of vertical splitting cracks and spalling had extended to a height of 400 mm above the foundation on the SW face of the column as shown in Figure 13(c), and the column had a residual drift of 1.6% in the S direction. Following EQ7, spalling and compressive damage on the S face were substantial as shown in Figure 13(d).

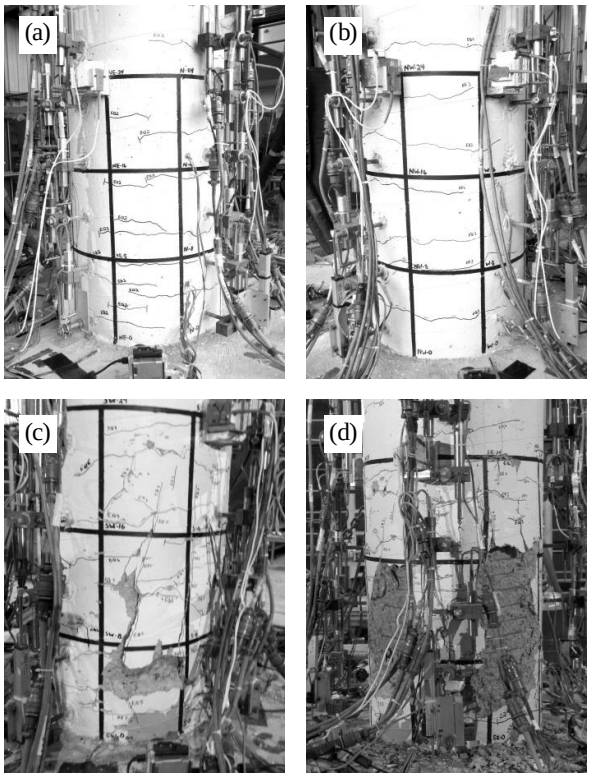

Figure 13 Damage to the Reference Column, (a) NE face after EQ2, (b) NW face after EQ2, (c) SE face after EQ6, and (d) S face after EQ7

5. SUMMARY

This test investigated the dynamic response of a 1/3 scale, rocking, post-tensioned HyFRC bridge column subjected to dynamic loading from scaled earthquake acceleration time history records (three components) on the shaking table. The column was designed to: (1) Minimize or eliminate the likelihood of residual column drifts for design level seismic drift demands up to 7%, (2) Limit inelastic compression damage at the rocking interface, and (3) Ensure that the post-tensioning remains elastic and prevent fracture of the continuous reinforcement at 7% drift.

The RPT HyFRC column consisted of a precast HyFRC end region up to a height of one column diameter (406 mm) containing headed reinforcing bars discontinuous at the column-foundation interface at a volumetric ratio of 1.5% and unbonded continuous reinforcing bars and post-tensioning strands at a volumetric ratio of $\rho_{l,eff}$ = 1.2%. The remainder of the column was cast with normal concrete. Smooth steel wire was used as shear and confinement reinforcement at a volumetric ratio of ρ_s = 0.9%. A reference column having similar geometry, lateral strength, and inertial mass, was also subjected to the same acceleration time histories as the RPT HyFRC column. This column had a volumetric ratio of longitudinal steel of ρ_l = 1.6% and contained the same A82 steel spiral at the same ratio as the RPT HyFRC column.

The test setup was identical in the two tests; accelerometers, linear potentiometers, displacement transducers, and strain gages measured column acceleration, displacement, and strain during testing. Reaction forces were measured with load cells fixed below the rigid foundation.

Seven earthquake tests with increasing ductility targets (in the reference column) were applied to both columns, and the RPT HyFRC column was also subjected to four additional tests.

5.1 Reduction in Residual Column Drifts

Similar peak drifts were imposed in the two columns by the EQ4, EQ5, and EQ6 (less than 20% difference) which targeted μ equal to four, four, and six, respectively, in the reference column. The RPT HyFRC column reached peak drifts of 4.3%, 6.2%, and 5.0% during these tests, but experienced residual drifts of only 0.1%, 0.1%, and 0.2%. The reference column reached peak drifts of 3.7%, 5.8%, and 6.1% during the same tests with residual drifts of 0.3%, 0.9%, and 1.6%. During EQ7, the reference column reached a peak drift of 10.8% due to the large residual of 1.6% after EQ6; following EQ7, the residual drift increased to 6.8%. The RPT HyFRC column showed residual drifts of less than 1% through the duration of testing, reaching peak drifts of 8.0%, 6.8%, 7.2%, 7.2%, and 8.8% with residuals of 0.4%, 0.4%, 0.6%, 0.6%, and 0.9% during EQ7 through EQ11.

5.2 Compressive Damage in the RPT HyFRC Column

The combination of discontinuous headed reinforcing bars and HyFRC in the precast end region prevented major compression damage which aided in preventing residual column drifts caused by damage at the rocking interface.

Measured peak strains over all tests in the discontinuous headed bars reached between 2% and 6% in compression yet buckling was not observed in any test. Spalling of the HyFRC in the precast end region was prevented. Some compressive cracks developed in early tests (Figure 10) on both sides of the column less than 75 mm above the top of the foundation; these cracks slowly propagated vertically as

splitting cracks as testing continued (Figure 11). Post-test inspection showed damage to the HyFRC was limited to the cover material (Figure 12). The spiral did not fracture, although compressive strains in the core material (as measured by strain gages on the headed bars) reached over 6%.

5.3 Behavior of the Unbonded Bars and PT Strands

Fracture of the unbonded bars was prevented for the first ten EQ tests; during EQ11, bars U1 and U4 fractured, likely due to low-cycle fatigue from prior tests. Prior to EQ11 the measured strain in bar U1 remained below 4% as uplift induced strains were spread over the unbonded length.

Losses in the initial PT force were less than 5% over the duration of testing and the force remained well below the expected yield load during testing.

6. CONCLUSIONS

The measured and observed experimental response of the RPT HyFRC column confirmed that the three main design objectives were successfully achieved. Several key observations were drawn from evaluation of the test:

i. Imposed drifts were successfully accommodated by rocking about the column-foundation interface rather than plastic hinge formation.

ii. The overturning resistance provided by the combination of unbonded PT strands and unbonded continuous reinforcing bars encouraged column re-centering behavior, even after yielding the unbonded bars. Residual drifts were significantly lower in the RPT HyFRC column compared to the reference column.

iii. The headed bars helped relieved compression in the HyFRC end region; significant inelastic yielding in compression was observed but buckling was prevented.

iv. Spalling was prevented by the HyFRC and most cracking was limited to below 200 mm from the top of the foundation. Damage to HyFRC was mostly restricted to the cover material.

Acknowledgements:

This project was funded by the Pacific Earthquake Engineering Research Center. The authors would like to acknowledge Bekaert, Headed Reinforcement Corporation, and Dywidag Systems International for their generous donations of material and equipment for this test series. Special thanks to the engineers and staff at the PEER Earthquake Simulator Laboratory for their advice and assistance during specimen construction and testing as well as to Drs. Matthew Schoettler and Vesna Terzic for managing the PEER Damage Resistant Re-centering Bridge Columns test series.

References:

Belleri, A., Schoettler, M. J., Restrepo, J. I., and Fleischman, R. B. (2013), "Dynamic Behavior of Rocking and Hybrid Cantilever Walls in a Precast Concrete Building," *ACI Structural Journal*, American Concrete Institute, accepted for publication Jan. 2013.

Billington, S. L. and Yoon, J. K. (2004), "Cyclic Response of Unbonded Posttensioned Precast Columns with Ductile Fiber-Reinforced Concrete," *Journal of Bridge Engineering*, American Society of Civil Engineers, **9**(4), 353-363.

Blunt, J. and Ostertag, C. P. (2009), "Deflection Hardening and Workability of Hybrid Fiber Composites," *ACI Materials Journal*, American Concrete Institute, **106**(3), 265-272.

California Department of Transportation (2006), "Caltrans Seismic Design Criteria Version 1.6," Sacramento, CA.

Cheng, C. T. (2008), "Shaking table tests of a self-centering designed bridge substructure," *Engineering Structures*, Elsevier, **30**, 3426-3433.

ElGawady, M., Booker, A. J., and Dawood, H. M. (2010), "Seismic Behavior of Posttensioned Concrete-Filled Fiber Tubes," *Journal of Composites for Construction*, American Society of Civil Engineers, **14**(5), 616-628.

Hewes, J. T. and Priestley, M. J. (2002), "Seismic Design and Performance of Precast Concrete Segmental Bridge Columns," *Report No. SSRP-2001/25*, University of California, San Diego.

Holden, T., Restrepo, J., and Mander, J. (2003), "Seismic Performance of Precast Reinforced and Prestressed Concrete Walls," *Journal of Structural Engineering*, American Society of Civil Engineers, **129**(3), 286-296.

Housner, G. W. (1963), "The Behavior of Inverted Pendulum Structures During Earthquakes," *Bulletin of the Seismological Society of America*, **53**(2), 403-417.

Jen, G., Trono, W., and Ostertag, C. P. (2012), "Self-consolidating HyFRC: Processing,, Properties and Applications," to be submitted.

Jeong, H. I., Sakai, J., and Mahin, S. A. (2008), "Shaking Table Tests and Numerical Investigation of Self-Centering Reinforced Concrete Bridge Columns," *PEER Report 2008/06*, Pacific Earthquake Engineering Research Center, Berkeley, CA.

Kwan, W. P. and Billington, S. L. (2003), "Unbonded Posttensioned Concrete Bridge Piers. I: Monotonic and Cyclic Analyses," *Journal of Bridge Engineering*, American Society of Civil Engineering, **8**(2), 92-101.

Kwan, W. P. and Billington, S. L. (2003), "Unbonded Posttensioned Concrete Bridge Piers. II: Seismic Analyses," *Journal of Bridge Engineering*, American Society of Civil Engineering, **8**(2), 102-111.

Kumar, P., Jen, G., Trono, W., Panagiotou, M., and Ostertag, C. P. (2011), "Self Compacting Hybrid Fiber Reinforced Composites for Bridge Columns," *PEER Report 2011/106*, Pacific Earthquake Engineering Research Center, Berkeley, CA.

Mander, J. B. and Cheng, C. T. (1997), "Seismic design of bridge piers based on damage avoidance design," *NCEER 97-0014*, National Center for Earthquake Engineering Research, Buffalo, NY.

Panagiotou, M., Kumar, P., Jen, G., Trono, W., and Ostertag, C. P. (2012), "Experimental Response of Hybrid Fiber Reinforced Concrete Bridge Columns with Novel Detailing of the Longitudinal Reinforcement," to be submitted.

Restrepo, J., and Guerrini, G. (2012). Personal Communication.

Sakai, J. and Mahin, S. A. (2004), "Analytical Investigations of New Methods for Reducing Residual Displacements of Reinforced Concrete Bridge Columns," *PEER Report 2004/02*, Pacific Earthquake Engineering Research Center, Berkeley, CA.

Trono, W., Jen, G., Moreno, D. M., Billington, S. L., and Ostertag, C. P. (2011), "Confinement and Tension Stiffening Effects in High Performance Self-consolidated Hybrid Fiber Reinforced Concrete Composites," *Proceedings, Sixth International Workshop on High Performance Fiber Reinforced Cement Composites*, Rilem, 245-252.

Vithani, A. R. and Gupta, K. C. (2002), "Estimation of Object Kinematics from Point Data," *Proceedings of DETC'02*, American Society of Mechanical Engineers, Montreal, Canada.